

# Tensile properties of as-cast and aged Pb-Sn-Ca alloys for positive grids of lead-acid batteries

Viktor O. Dzenzerskiy, Serhii V. Tarasov, Olena V. Sukhova\*, Dmytro O. Redchyts, Volodymyr A. Ivanov

*Institute of Transport Systems and Technologies of the National Academy of Sciences of Ukraine,  
5 Pysarzhevsky St., Dnipro 49005, Ukraine*

Received 4 April 2024, received in revised form 26 April 2024, accepted 24 May 2024

## Abstract

This work determined the microstructure and tensile properties of low-calcium Pb-Sn-Ca alloys (with a tin-to-calcium content ratio ranging from 18.4 to 23.5) used to produce positive lead-acid battery grids. Natural aging during storage under atmospheric conditions resulted in a breakdown of the supersaturated alpha-lead solid solution, with  $(\text{Pb},\text{Sn})_3\text{Ca}$  and  $\text{Sn}_3\text{Ca}$  strengthening particles precipitating. A noticeable change in grain size was not observed in the tested alloys aged for 32 days. The Pb-Sn-Ca alloys age-strengthened rapidly after casting, requiring 32 days to reach an average of 2.7, 4.9, and 1.3 times greater ultimate tensile strength, yield strength, and Young's modulus, respectively. The data obtained showed that the prolongation of aging time produced stronger and stiffer materials, but the average elongation of the alloys became 2.4 times lower. Age-strengthening mainly occurs during the first 15 days of natural aging.

**Key words:** lead-acid batteries, positive grids, lead-tin-calcium alloys, natural aging, stress-strain diagrams, tensile properties

## 1. Introduction

Many different electrical energy storage technologies are available that can be suitable for renewable energy storage and backup power applications. At a commercial level, energy storage in off-grid renewable energy systems is currently dominated by lead-acid batteries [1–3]. These batteries are a relevant choice due to their good characteristics in terms of safety, performance, and compact size [4–6]. Besides, lead-acid batteries are very cost-competitive, while their disadvantages are not a serious setback for use in power supply systems. The main elements of the lead-acid battery are the metal grids and the active material. The positive battery grid is important in constraining the active substances. As a core component of lead-acid batteries, the positive grid also plays a major role in collecting current.

Maintenance-free batteries generally use lead-calcium alloys as the materials of choice for positive grids [7–9]. Despite the improved processing, positive plates

produced from lead-calcium grids suffer from reduced cycle life, active material shedding, low charge acceptance, etc. Poor cycle life results in premature capacity loss for battery grids produced from lead-calcium alloys.

Tin additions have been shown to increase mechanical properties, reduce the tendency towards passivation, increase corrosion resistance, and impart stability to grids produced from Pb-Ca alloys [10–15]. The Pb-Sn-Ca alloys for positive grids usually have low calcium and moderate tin content. Despite their high corrosion resistance, these materials create problems in battery manufacturing [16]. Conventionally cast grids are extremely difficult to handle because of their low mechanical properties.

Due to age-hardening processes, lead-tin-calcium alloys produce higher mechanical properties by precipitating a highly dispersed second phase into the alpha-lead matrix [17–20]. Aging is the most widespread method to improve the performance of lead-based alloy systems like Pb-Sn-Ca. The very low calcium

\*Corresponding author: tel.: +38(097)9394571; e-mail address: [sukhovaya@ukr.net](mailto:sukhovaya@ukr.net)

Table 1. Tensile properties of as-cast Pb-Sn-Ca alloys

Casting No.	Ca (wt.%)	Sn (wt.%)	Sn/Ca	$\sigma_U$ (MPa)	$\gamma$ (%)
574	0.057	1.05	18.42	20.12	33.61
457	0.056	1.05	18.75	18.78	35.81
539	0.053	1.07	20.19	19.99	32.24
501	0.052	1.07	20.58	19.56	36.26
517	0.053	1.10	20.75	19.94	35.31
667	0.051	1.06	20.78	20.04	33.38
475	0.053	1.11	20.94	19.79	35.00
499	0.052	1.10	21.15	20.36	33.36
498	0.049	1.14	23.27	19.95	33.95
472	0.048	1.13	23.54	19.77	36.62
<b>average</b>	<b>0.052</b>	<b>1.09</b>	<b>20.84</b>	<b>19.83</b>	<b>34.55</b>

contents produce soft grids that harden slowly and require artificial aging at high temperatures to obtain adequate mechanical properties. The typical microstructure of these positive grid alloys consists of lead grains with a dispersion of  $Pb_3Ca$  or  $(Pb,Sn)_3Ca$  particles, the amount and distribution depending on the tin-to-calcium content ratio (Sn/Ca) [21–25]. To produce more stable and stronger precipitate particles of  $Sn_3Ca$ , a Sn/Ca ratio of at least 9 is needed since the continuous precipitation of the  $Pb_3Ca$  or  $(Pb,Sn)_3Ca$  compounds occurs preferentially. So, alloys with a higher Sn/Ca ratio must force all the calcium to precipitate as  $Sn_3Ca$  instead of  $Pb_3Ca$  or mixed  $(Pb,Sn)_3Ca$  precipitates.

Thus, selecting appropriate levels of elements for the battery-positive grids involves considerations of production capability, economic feasibility, and the mechanical and electrochemical properties of the alloys. Previous studies have shown that the contents of tin and calcium are the main factors influencing the microstructure and mechanical properties of Pb-Sn-Ca alloys. The optimized contents of Sn and Ca in positive grid alloys are believed to be above about 1.0 wt.% and about 0.05 wt.% level, respectively [1–3]. These cast alloys with a high ratio of tin-to-calcium content (exceeding 18) utilized in positive grids have a chemical composition optimized for processing.

Grid manufacturing processes require sufficient grid tensile properties in lead-acid batteries for efficient processing of grids through automatic pasting machines and other handling equipment. However, most investigations have focused on composition ranges, corrosion properties, strengthening mechanisms, hardness and/or resistivity measurements, etc. Unfortunately, information regarding the tensile properties of Pb-Sn-Ca grid alloys with a tin-to-calcium content ratio exceeding 18 is incomplete and, at times, contradictory. Therefore, this research aims to determine the microstructure and tensile properties of the cast Pb-Sn-Ca alloys with a tin-to-calcium content ratio between 18.4 and 23.5 as a function of

aging time during storage under atmospheric conditions.

## 2. Materials and methods

The investigated Pb-Sn-Ca alloys were cast in the C.O.S. melt pot of the production line for positive grids of lead-acid batteries of BM Company (Austria) at Westa Corp. (City of Dnipro, Ukraine). The temperature of the melt in the pot was kept at  $455 \pm 5^\circ C$ . The molten metal was poured into a casting mold preheated up to  $75 \pm 5^\circ C$  and left to cool to room temperature. The temperature was measured by a chromel-alumel thermocouple with a standard error of  $\pm 5^\circ C$ . The chemical composition of the alloys was determined by atomic absorption spectroscopy using the ARL 3460 device. Tin content in the Pb-Sn-Ca alloys was checked to be 1.05–1.14 wt.%, calcium content – 0.048–0.057 wt.%, lead – the balance (see Table 1). Major impurities consisted of Bi and Al (in descending order), with total impurities content less than 0.02 wt.%.

After casting, the specimens were left to age under atmospheric conditions for 32 days before studying their microstructure in a Neophot light-optical microscope. Alloys samples were mechanically and electrochemically polished before metallographic testing [23, 25]. The size of the grains was measured by quantitative metallography on an Epiquant structural analyzer with a standard error not exceeding 4%.

The tensile tests were carried out at room temperature in the TIRAtest 2300 universal testing machine. Standard flat specimens with a total length of 6.0 cm, a gauge length of 4.5 cm, and a thickness of 0.3 cm were prepared. The crosshead speed was  $10 \text{ mm min}^{-1}$ . The tensile force was applied stepwise with a step of 100 N until the stress part of the stress-strain diagrams started falling back down slowly. The nominal stress ( $P_H$ ) and strain elongation ( $\Delta l/l$ ) were fixed digitally and plotted. The ultimate

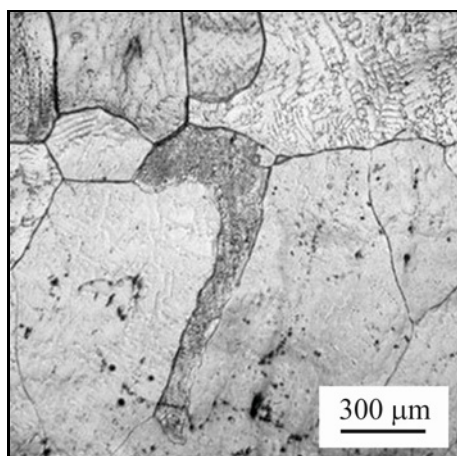


Fig. 1. Typical microstructure of as-cast Pb-Sn-Ca alloys.

tensile strength ( $\sigma_U$ ), yield strength ( $\sigma_Y$ ), Young's modulus ( $Y$ ), and elongation ( $\gamma$ ) were calculated 1 day after casting and then at intervals of 2–5 days for 32 days. Each determined value of tensile properties corresponded to the mean of six measurements. The average uncertainty of measurements did not exceed approximately 5%.

### 3. Results and discussion

The typical microstructure of low-calcium Pb-Sn-Ca alloys, as observed in the as-cast specimens, is given in Fig. 1. The alpha-lead grains are well-defined and have  $387 \pm 16 \mu\text{m}$  in size. Such a coarse-grained structure is beneficial for minimizing intergranular corrosion [26–29]. In the studied alloys, fine intermetallic precipitates are also observed to form within the grains immediately after casting. Previous investigations [17–25] show that tin is segregated in intercellular regions, and the calcium precipitation is converted from cellular to continuous precipitation to form  $(\text{Pb,Sn})_3\text{Ca}$  phase. This is followed by several discontinuous transformations to form  $\text{Sn}_3\text{Ca}$  precipitates.

The tensile properties of the Pb-Sn-Ca alloys determined immediately after casting are shown in Table 1. As seen, there are no clear dependences of the ultimate tensile strength ( $\sigma_U$ ) or relative elongation ( $\gamma$ ) on the tin-to-calcium ratio ( $\text{Sn}/\text{Ca}$ ) increasing in the range between 18.42 and 23.54. The effects of rising tin or calcium contents are irregular as well. The ultimate tensile strength values increase from 18.78 to 20.36 MPa, and those of elongation increase from 32.24 to 36.62%. Such spread of values is most likely connected with variations in the casting procedure since no connection with impurities content is also revealed.

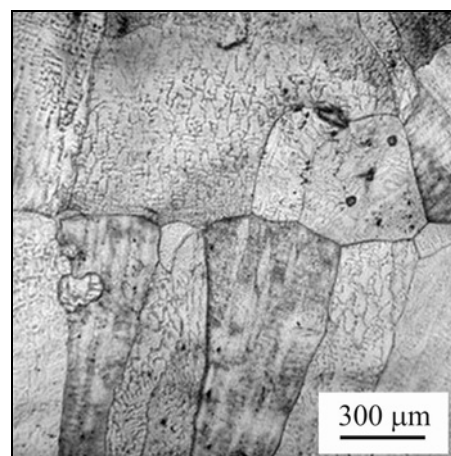


Fig. 2. Typical microstructure of Pb-Sn-Ca alloys aged for 32 days.

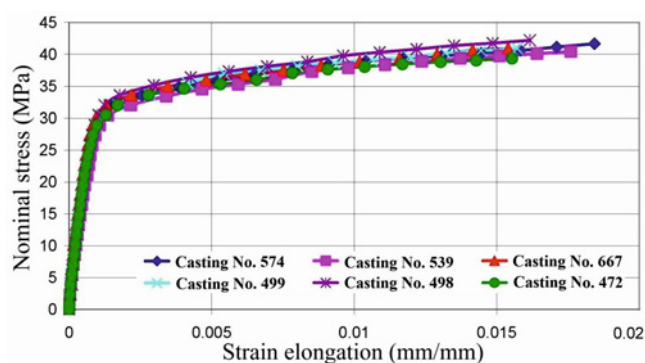


Fig. 3. Stress-strain diagrams of Pb-Sn-Ca alloys aged for 27 days.

After casting, the Pb-Sn-Ca alloys are stored under atmospheric conditions where they are naturally aged. The microstructure shown in Fig. 2 indicates that the average grain size remains almost unchanged, staying within the measurement error of approximately 4% after aging for 32 days. So, the grain structure of the alloys is stable, with very little change in size throughout the studied aging period.

The stress-strain diagrams show a good convergence of tensile test results for specimens taken from different castings and aged for 27 days (see Fig. 3). All diagrams have a linear elastic part where the nominal stress and strain are proportional and a gradually rising portion where specimens undergo plastic deformation.

Considering that stress-strain curves for specimens out of different castings closely resemble each other, data obtained from tensile tests can be averaged, and the average stress-strain diagram can be plotted as a function of aging time, as shown in Fig. 4. With aging time prolonging, a slope of the curves in their linear range increases, which indicates the improve-

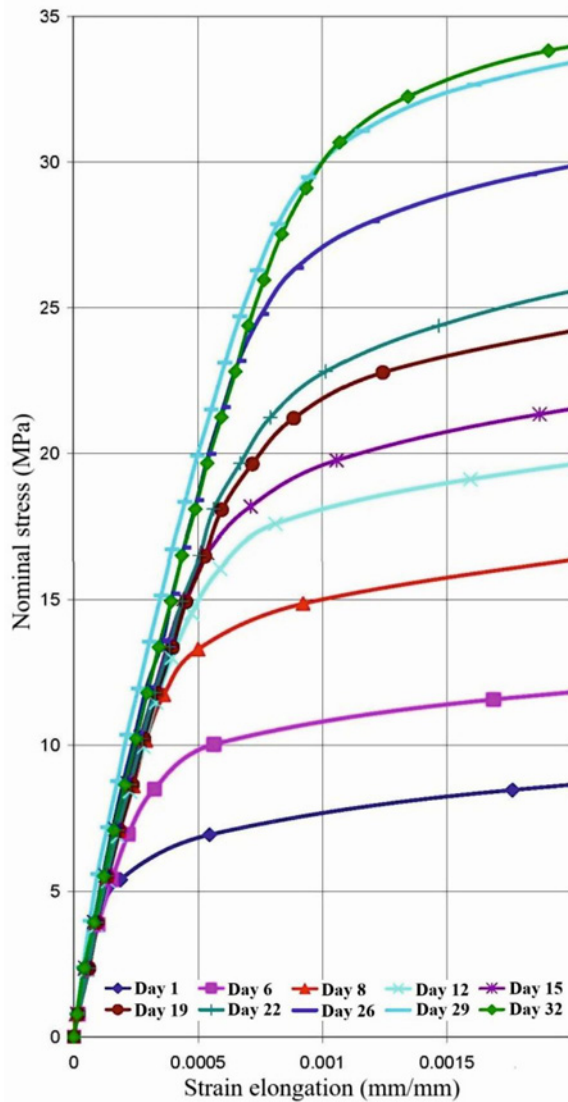


Fig. 4. Stress-strain diagrams of Pb-Sn-Ca alloys aged for 1–32 days.

ment of elastic properties. All plots display a larger linear part where the stress-strain relationship is proportional, so the nominal stress at which alloys deform plastically increases. The higher lift of the stress-strain curves evidences that the aged Pb-Sn-Ca alloys be-

come stronger. These observations are confirmed by values of calculated tensile properties presented in Table 2.

After 32 days of natural aging, ultimate tensile strength ( $\sigma_U$ ) and yield strength ( $\sigma_Y$ ) are 2.7 and 4.9 times greater, respectively. Young's modulus ( $Y$ ) increases by 30 % while elongation becomes 2.4 times lower (Table 2). Mechanical properties of the Pb-Sn-Ca alloys change at a higher rate during the first 15 days of aging. This indicates that after this period, the precipitation rate slows down.

As mentioned above, ultimate tensile strength, yield strength, and Young's modulus show an increasing trend with the aging time extending, which evidences that the tin-to-calcium content ratio of the studied Pb-Sn-Ca alloys allows producing not only  $(\text{Pb,Sn})_3\text{Ca}$  strengthening particles but more stable and stronger  $\text{Sn}_3\text{Ca}$  precipitates, amount and density of which are sufficient to elevate strength and stiffness significantly.

The increase in the yield strength is greater than that in the ultimate tensile strength of the aged Pb-Sn-Ca alloys. This is consistent with the fact that the yield strength is more influenced by the strengthening precipitates produced during aging, which constitute an effective obstacle for inhibiting the dislocation and grain boundary movement [30–32].

The lower yield strength values compared with those of ultimate tensile strength can be attributed to the precipitation and growth of the strengthening phases, which consume alloying elements in the super-saturated alpha-lead solid solution. As a result, the distribution of these elements is less effective in blocking the motion of dislocations within the lead grains and thus weakens the strengthening effects.

Aging increases strength and stiffness to some extent but results in a loss of ductility. This is due to the higher volume fraction of precipitates formed on the dislocations. It is believed that both the resistance to dislocation motion and the promotion of inhomogeneous dislocation multiplication by the precipitates become higher. As a result, dislocations are less uniformly distributed, and deformation is localized, causing a decrease in elongation.

The faster change in tensile properties during the

Table 2. Averaged values of tensile properties of Pb-Sn-Ca alloys vs. aging time

Property	Aging time (days)				
	1	8	15	26	32
$\sigma_U$ (MPa)	20.1	30.2	45.0	50.1	53.6
$\sigma_Y$ (MPa)	5.4	12.2	19.4	22.0	26.3
$Y$ (GPa)	15.8	16.9	20.1	20.5	20.6
$\gamma$ (%)	29.0	21.5	16.8	14.3	12.0

first 15 days of aging can be related to the rapid precipitation of the  $\text{Sn}_3\text{Ca}$  strengthening particles and their growth. The slower change in the later aging stage is believed to be mainly attributed to the saturation of precipitation and the decrease in precipitation rate.

#### 4. Conclusions

The investigated cast Pb-Sn-Ca alloys cooled from the melt kept at  $455 \pm 5^\circ\text{C}$  and poured in a casting mold preheated up to  $75 \pm 5^\circ\text{C}$  acquire mechanical properties due to the formation of a supersaturated lead-rich solid solution. Such casting conditions produce a coarse-grained structure with dispersed  $(\text{Pb},\text{Sn})_3\text{Ca}$  and  $\text{Sn}_3\text{Ca}$  precipitate particles. Upon subsequent storage under atmospheric conditions (natural aging), the alloys approach equilibrium by further precipitation of these strengthening phases from the lead-rich matrix.

During 32 days of storage, the precipitation processes are not accompanied by noticeable changes in grain size but strengthen the alloys, causing a significant increase in the average values of ultimate tensile strength, yield strength, and Young's modulus of up to 2.7, 4.9, and 1.3 times, respectively, but the alloys undergo a loss in average elongation by 2.4 times.

Natural aging for 32 days helps to increase the alloy's strength and correspondingly eases plant handling of the positive grids. The studied Pb-Sn-Ca alloys do not require longer aging time to stabilize their microstructure and mechanical properties since those change at a higher rate during the first 15 days of aging.

#### References

- [1] J. Jung, L. Zhang, J. Zhang, *Lead-Acid Battery Technologies: Fundamentals, Materials, and Applications*, CRC Press, Boca Raton, 2015. <https://doi.org/10.1201/b18665>
- [2] S. Guruswamy, *Engineering Properties and Applications of Lead Alloys*, CRC Press, New York, 2000. <https://doi.org/10.1201/9781482276909>
- [3] D. A. J. Rand, T. Moseley, J. Garche, C. D. Parker, *Valve-Regulated Lead-Acid Batteries*, Elsevier, Amsterdam, 2004. <https://doi.org/10.1016/B978-0-444-50746-4.X5000-4>
- [4] V. O. Dzenzerskiy, S. V. Tarasov, O. V. Sukhova, V. A. Ivanov, Evolution of mechanical properties of Pb-Sb-Sn-As-Se grid alloys for lead-acid batteries during natural ageing, *East Eur. J. Phys.* 4 (2023) 182–188. <https://doi.org/10.26565/2312-4334-2023-4-21>
- [5] V. O. Dzenzerskiy, S. V. Tarasov, D. O. Redchyt, V. A. Ivanov, O. V. Sukhova, Mechanical properties of Pb-Sn-Ba grid alloys for lead-acid batteries produced by melt spinning technology, *J. Nano-Electron. Phys.* 16 (2024) 01003. [https://doi.org/10.21272/jnep.16\(1\).01003](https://doi.org/10.21272/jnep.16(1).01003)
- [6] V. O. Dzenzerskiy, S. V. Tarasov, O. V. Sukhova, V. A. Ivanov, Effects of composition and cooling rate on mechanical properties of Pb-Sb-Sn-As grid alloys, *Rom. J. Phys.* 69 (2024) 605. <https://doi.org/10.59277/RomJPhys.2024.69.605>
- [7] E. Gullian, L. Albert, J. L. Caillerie, New lead alloys for high-performance lead-acid batteries, *J. Power Sources* 116 (2003) 185–192. [https://doi.org/10.1016/S0378-7753\(02\)00705-X](https://doi.org/10.1016/S0378-7753(02)00705-X)
- [8] D. A. J. Rand, D. P. Boden, C. S. Lakshmi, R. R. Nelson, R. D. Prengaman, Manufacturing and operational issues with lead-acid batteries, *J. Power Sources* 107 (2002) 280–300. [https://doi.org/10.1016/S0378-7753\(01\)01083-7](https://doi.org/10.1016/S0378-7753(01)01083-7)
- [9] K. Sawai, Y. Tsuboi, Y. Okada, M. Shiomi, S. Osumi, New approach to prevent premature capacity loss of lead-acid battery in cycle use, *J. Power Sources* 179 (2008) 799–807. <https://doi.org/10.1016/j.jpowsour.2007.12.106>
- [10] E. Rocca, G. Bourguignon, J. Steinmetz, Corrosion management of PbCaSn alloys in lead-acid batteries: Effect of composition, metallographic state and voltage conditions, *J. Power Sources* 161 (2006) 666–675. <https://doi.org/10.1016/j.jpowsour.2006.04.140>
- [11] M. T. Wall, Y. Ren, T. Hesterberg, T. Ellis, M. L. Young, Effects of micro-alloying with lead for battery grid material, *J. Energy Storage* 55 (2022) 105569. <https://doi.org/10.1016/j.est.2022.105569>
- [12] D. Slavkov, B. S. Haran, B. N. Popov, F. Fleming, Effect of Sn and Ca doping on the corrosion of Pb anodes in lead acid batteries, *J. Power Sources* 112 (2002) 199–208. [https://doi.org/10.1016/S0378-7753\(02\)00368-3](https://doi.org/10.1016/S0378-7753(02)00368-3)
- [13] H. Li, W. X. Guo, H. Y. Chen, D. E. Finlow, H. W. Zhou, C. L. Dou, G. M. Xiao, S. G. Peng, W. W. Wei, H. Wang, Study on the microstructure and electrochemical properties of lead-calcium-tin-aluminum alloys, *J. Power Sources* 191 (2009) 111–118. <https://doi.org/10.1016/j.jpowsour.2008.10.059>
- [14] R. K. Shervedani, A. Z. Isfahani, R. Khodavisy, A. Hatefi-Mehrjardi, Electrochemical investigation of the anodic corrosion of Pb-Ca-Sn-Li grid alloy in  $\text{H}_2\text{SO}_4$  solution, *J. Power Sources* 164 (2007) 890–895. <https://doi.org/10.1016/j.jpowsour.2006.10.105>
- [15] Y. B. Zhou, C. X. Yang, W. F. Zhou, H. T. Liu, Comparison of Pb-Sm-Sn and Pb-Ca-Sn alloys for the positive grids in a lead acid battery, *J. Alloys Compd.* 365 (2004) 108–111. [https://doi.org/10.1016/S0925-8388\(03\)00649-2](https://doi.org/10.1016/S0925-8388(03)00649-2)
- [16] R. D. Prengaman, Wrought lead-calcium-tin alloys for tubular lead-acid-battery grids, *J. Power Sources* 53 (1995) 207–214. [https://doi.org/10.1016/0378-7753\(94\)01975-2](https://doi.org/10.1016/0378-7753(94)01975-2)
- [17] C. S. Lakshmi, J. E. Manders, D. M. Rice, Structure and properties of lead-calcium-tin alloys for battery grids, *J. Power Sources* 73 (1998) 23–29. [https://doi.org/10.1016/S0378-7753\(98\)00018-4](https://doi.org/10.1016/S0378-7753(98)00018-4)
- [18] M. Dehmas, A. Maître, J. B. Richir, P. Archambault, Kinetics of precipitation hardening in Pb-0.08wt.%Ca-zwt.%Sn alloys by in situ resistivity measurements, *J. Power Sources* 159 (2006) 721–727. <https://doi.org/10.1016/j.jpowsour.2005.07.094>

- [19] C. Camurri, C. Carrasco, O. Prat, R. Mangalaraja, A. Pagliero, R. Colas, Study of precipitation hardening in lead calcium tin anodes for copper electro-winning, *Mater. Sci. Technol.* 26 (2010) 210–214. <https://doi.org/10.1179/174328409x443245>
- [20] A. Maitre, G. Bourguignon, G. Medjahdi, E. McRae, M. H. Mathon, Experimental study of L12 phase precipitation in the Pb-0.08wt.%Ca-2.0wt.%Sn alloy by resistivity and SANS measurements, *Scr. Mater.* 50 (2004) 685–689. <https://doi.org/10.1016/j.scriptamat.2003.11.013>
- [21] F. Rossi, M. Lambertin, L. Delfaut-Durut, A. Maitre, M. Vilasi, Influence of the cooling rate on the ageing of lead-calcium alloys, *J. Power Sources* 188 (2009) 296–300. <https://doi.org/10.1016/j.jpowsour.2008.11.049>
- [22] H. Tsubakino, R. Nozato, A. Yamamoto, Precipitation in Pb-0.04Ca-1.2Sn alloy, *Scr. Mater.* 26 (1992) 1681–1685. [https://doi.org/10.1016/0956-716X\(92\)90533-K](https://doi.org/10.1016/0956-716X(92)90533-K)
- [23] L. Bouriden, J. P. Hilger, J. Hertz, Discontinuous and continuous hardening processes in calcium and calcium-tin micro-alloyed lead: influence of ‘secondary-lead’ impurities, *J. Power Sources* 33 (1991) 27–59. [https://doi.org/10.1016/0378-7753\(91\)85046-Y](https://doi.org/10.1016/0378-7753(91)85046-Y)
- [24] Y. A. Yassine, M. Lakhali, N. Labchir, E. Zantalla, E. Saad, M. Sannad, Kinetic study of the ageing and overageing of alloy Pb0.058%Ca0.12%Sr1.09%Sn for battery grids, *Coat.* 13 (2023) 1534. <https://doi.org/10.3390/coatings13091534>
- [25] J. Hilger, How to decrease overageing in Pb-Ca-Sn alloys, *J. Power Sources* 72 (1998) 184–188. [https://doi.org/10.1016/s0378-7753\(97\)02711-0](https://doi.org/10.1016/s0378-7753(97)02711-0)
- [26] O. V. Sukhova, V. A. Polonskiy, Structure and corrosion of quasicrystalline cast Al-Co-Ni and Al-Fe-Ni alloys in aqueous NaCl solution, *East Eur. J. Phys.* 3 (2020) 5–10. <https://doi.org/10.26565/2312-4334-2020-3-01>
- [27] R. D. Prengaman, Challenges from corrosion-resistant grid alloys in lead acid battery manufacturing, *J. Power Sources* 95 (2001) 224–233. [https://doi.org/10.1016/S0378-7753\(00\)00620-0](https://doi.org/10.1016/S0378-7753(00)00620-0)
- [28] O. V. Sukhova, V. A. Polonskiy, K. V. Ustinova, Corrosion-electrochemical properties of quasicrystalline Al-Cu-Fe-(Si,B) and Al-Ni-Fe alloys in NaCl solution, *Voprosy Khimii i Khimicheskoi Tekhnologii* 124 (2019) 46–52. (in Ukrainian) <https://doi.org/10.32434/0321-4095-2019-124-3-46-52>
- [29] S. I. Ryabtsev, V. A. Polonskiy, O. V. Sukhova, Corrosion resistance of alloys of the Al-Cu-Fe-(Si,B) system in mineralized saline and acid solutions, *Mater. Sci.* 56 (2020) 263–272. <https://doi.org/10.1007/s11003-020-00428-8>
- [30] O. V. Sukhova, Structure and properties of Fe-B-C powders alloyed with Cr, V, Mo or Nb for plasma-sprayed coatings, *Probl. At. Sci. Technol.* 128 (2020) 77–83. <https://doi.org/10.46813/2020-128-077>
- [31] V. Lozynskiy, B. Trembach, M. M. Hossain, M. H. Kabir, Y. Silchenko, M. Krabata, K. Sadoviy, O. Kolomiitse, L. Ropyak, Prediction of phase composition and mechanical properties of Fe-Cr-C-B-Ti-Cu hardfacing alloys: Modeling and experimental validations, *Heliyon* 10 (2024) e25199. <https://doi.org/10.1016/j.heliyon.2024.e25199>
- [32] O. V. Sukhova, Solubility of Cu, Ni, Mn in boron-rich Fe-B-C alloys, *Phys. Chem. Solid St.* 22 (2021) 110–116. <https://doi.org/10.15330/pcss.22.1.110-116>